Published in final edited form as:
Circulation. 2011 March 8; 123(9): 979–988. doi:10.1161/CIRCULATIONAHA.110.006437.

Disrupted Junctional Membrane Complexes and Hyperactive Ryanodine Receptors Following Acute Junctophilin Knockdown in Mice

Ralph J. van Oort, PhD[1,*], **Alejandro Garbino, PhD**[1,*], **Wei Wang, PhD**[1,*], **Sayali S. Dixit, PhD**[1], **Andrew P. Landstrom, BS**[2], **Namit Gaur, MS**[3], **Angela C. De Almeida, MS**[1], **Darlene G. Skapura, BS**[1], **Yoram Rudy, PhD**[3], **Alan R. Burns, PhD**[4], **Michael J. Ackerman, MD PhD**[2], and **Xander H.T. Wehrens, MD PhD**[1,5]

[1] Dept. of Molecular Physiology and Biophysics, Baylor College of Medicine, Houston, Texas, 77030, USA

[2] Depts. of Molecular Pharmacology & Experimental Therapeutics, Medicine, and Pediatrics, Mayo Clinic, Rochester, Minnesota, 55905, USA

[3] Cardiac Bioelectricity and Arrhythmia Center, Washington University, St. Louis, Missouri, 63130, USA

[4] College of Optometry, University of Houston, Houston, 77204, Texas, USA

[5] Dept. of Medicine - Division of Cardiology, Baylor College of Medicine, Houston, Texas, 77030, USA

Abstract

Background—Excitation-contraction coupling in striated muscle requires proper communication of plasmalemmal voltage-activated Ca^{2+} channels and Ca^{2+} release channels on sarcoplasmic reticulum (SR) within junctional membrane complexes (JMCs). Whereas previous

Correspondence: Xander H.T. Wehrens, MD PhD Dept. of Molecular Physiology and Biophysics Baylor College of Medicine One Baylor Plaza, BCM335 Houston, TX 77030, United States Tel 713-798-4261; Fax 713-798-3475; wehrens@bcm.edu.
*Equal contributions.

Subject Codes: [130] Animal models of human disease, [136] Calcium cycling/excitation-contraction coupling, [145] Genetically altered mice, [148] Heart failure - basic studies, [152] Ion channels/membrane.

DISCLOSURES None.

Clinical Summary

Impaired cardiac muscle contraction is a hallmark of congested heart failure. At the cellular level, excitation-contraction coupling requires proper communication of plasmalemmal voltage-gated Ca^{2+} channels and Ca^{2+} release channels on the sarcoplasmic reticulum within junctional membrane complexes (JMCs). Disruption of the JMC structure is commonly seen in heart failure, and thought to contribute to contractile failure. Junctophilin-2 has recently been proposed to provide a structural connection between the plasma membrane and sarcoplasmic reticulum within the JMC, although its function has remained unclear due to the lack of adequate animal models. We have developed a novel approach to conditionally reduce JPH2 protein levels using RNA interference. Our studies revealed that acute knockdown of JPH2 leads to loss of cardiac contractility and heart failure in mice. JPH2 was found to determining the spacing between the plasmalemma and SR membrane, in addition to being required for the structural integrity of JMCs within myocytes. Computational analysis provided further quantitative insights into the relative importance of each of these subcellular defects related to impaired excitation-contraction coupling. Finally, our data showed that JPH2 associates with and facilitates RyR2 inactivation, thereby preventing diastolic SR Ca^{2+} leak that could promote heart failure. Taken together, our studies suggest that downregulation of JPH2 could play an important role in the development of contractile dysfunction in heart failure.

studies revealed a loss of JMCs and embryonic lethality in germ-line junctophilin-2 (JPH2) knockout mice, it has remained unclear whether JPH2 plays an essential role in JMC formation and the Ca^{2+}-induced Ca^{2+} release process in the heart. Our recent work demonstrated loss-of-function mutations in JPH2 in patients with hypertrophic cardiomyopathy.

Methods and Results—To elucidate the role of JPH2 in the heart, we developed a novel approach to conditionally reduce JPH2 protein levels using RNA interference. Cardiac-specific JPH2 knockdown resulted in impaired cardiac contractility, which caused heart failure and increased mortality. JPH2 deficiency resulted in loss of excitation-contraction coupling gain, precipitated by a reduction in the number of JMCs and increased variability in the plasmalemma-SR distance.

Conclusions—Loss of JPH2 had profound effects on Ca^{2+} release channel inactivation, suggesting a novel functional role for JPH2 in regulating intracellular Ca^{2+} release channels in cardiac myocytes. Thus, our novel approach of cardiac-specific shRNA-mediated knockdown of junctophilin-2 has uncovered a critical role for junctophilin in intracellular Ca^{2+} release in the heart.

Keywords

Calcium; excitation-contraction coupling; heart failure; junctophilin; sarcoplasmic reticulum

BACKGROUND

Excitation-contraction (EC) coupling is the fundamental mechanism by which depolarization of the voltage-gated Ca^{2+} channels (VGCCs) in the plasmalemma triggers a much greater release of Ca^{2+} from the sarcoplasmic reticulum (SR) via type 2 ryanodine receptors (RyR2), a process known as Ca^{2+}-induced Ca^{2+} release (CICR).[1] This Ca^{2+} release amplification depends on the organization of VGCC and RyR2 within junctional membrane complexes (JMCs), also known as calcium release units (CRUs).[2] Disruption of JMC structure, as seen in heart failure, profoundly affects CICR and thus cardiac muscle contractility.3

The molecular mechanisms involved in organizing Ca^{2+} channels within the JMC remain poorly understood. One family of proteins, known as junctophilins (JPHs), has been proposed to provide a structural bridge between the plasmalemma and SR, thereby potentially ensuring approximation of VGCC and RyR2.4 Junctophilin-2 (JPH2) is the major cardiac isoform among the four JPH isoforms, which are expressed within JMCs of all excitable cell types.5 JPH proteins comprise eight N-terminal ‘membrane occupation and recognition nexus’ (MORN) domains, a space-spanning alpha helix, and a C-terminal ‘transmembrane domain’ (TMD). The MORN domains mediate binding to the plasmalemma, while the hydrophobic TMD is anchored into the SR membrane.6

The role of junctophilin in myocytes has remained unclear due to the lack of adequate animal models. Mice deficient in *JPH1*, the major skeletal muscle isoform, suffer from muscle abnormalities and perinatal death.[7] Genetic ablation of *JPH2* results in embryonic lethality, most likely due to absence of cardiac contractility around embryonic day 10.5.[4] Therefore, the physiological role of JPH2 in the adult heart remains to be elucidated. In recent studies, we and another group have identified missense mutations in *JPH2* in patients with hypertrophic cardiomyopathy.[8, 9] Moreover, decreased JPH2 expression was observed in a rat model of aortic stenosis and mouse models of hypertrophic and dilated cardiomyopathy.[10, 11] However, it remains to be determined whether downregulation of JPH2 is a mere response to heart failure, or actually precipitates disease progression. Again,

unraveling these questions has thus far been greatly hampered by the lack of a suitable animal model.

To circumvent the embryonic lethality associated with conventional genetic deletion of *JPH2* we generated a novel transgenic mouse model that allows inducible cardiac-specific knockdown of JPH2 using RNA interference. We demonstrated that JPH2 deficiency is associated with the development of acute heart failure due to a loss of JMCs and reduced CICR. The CICR process was impaired due to reduced co-localization and functional coupling of VGCC and RyR2, without affecting expression levels. Moreover, loss of JPH2 impaired proper RyR2 inactivation, suggesting previously unrecognized roles for JPH2 in cardiac muscle, and directly linking JPH2 deficiency to contractile dysfunction in failing hearts.

METHODS

Please refer to the online data supplement for more detailed Methods.

Generation of Transgenic Mice

The generation of mice with cardiac-specific inducible shRNA-mediated knockdown of JPH2 is described in detail in the online-only Data Supplement.

Northern Blot and RT-PCR

Detailed methods are provided in the expanded Methods section (see online-only Data Supplement).

Western Blotting and Co-immunoprecipitation

Western blotting and Co-immunoprecipitation was performed as described in detail previously.[12]

Immunohistochemistry and Histology

Detailed methods are provided in the online-only Data Supplement.

Transthoracic Echocardiography

Mice were anesthetized using 1-2.0% isoflurane in 95%. Cardiac function was assessed using M-mode echocardiograms acquired with a VisualSonics VeVo 770 Imaging System (VisualSonics, Toronto, Canada), as described.[13]

Electrophysiology and Ca^{2+} Imaging

Detailed methods are provided in the online-only Data Supplement.

Electron Microscopy

Detailed methods are provided in the online-only Data Supplement.

Computational Model

Detailed methods are provided in the online-only Data Supplement.

Statistical Analysis

Data are expressed as mean ± SEM. Statistical significance of differences between experimental groups was compared using Student's *t*-test, one-way ANOVA with pairwise multiple comparisons performed using the Student-Newman-Keuls method as appropriate. If

results failed a normality test, the Wilcoxon rank sum or Kruskal-Wallis tests were used, as appropriate. A value of $P<0.05$ was considered statistically significant.

RESULTS

Cardiac-specific, Inducible JPH2 Knockdown Using RNA Interference

To circumvent embryonic lethality associated with germline JPH2 knockout we developed a novel approach for inducible cardiac-specific JPH2 knockdown. We first cloned 4 candidate short hairpin RNA (shRNA) oligonucleotides targeting different regions in mouse *JPH2* and tested the knockdown efficiency *in vitro* (Supplemental Fig. 1a). Western blot analysis demonstrated efficient knockdown for 3 JPH2-shRNA constructs (Supplemental Fig. 1b). The most efficient oligonucleotide (#2) was used to generate a conditional JPH2 knockdown (shJPH2) mouse. shJPH2 mice harbor a transgene composed of the JPH2 shRNA sequence downstream of a U6 promoter, which is inactive due to the insertion of a loxP flanked *neo* cassette.[14] To ensure cardiac-specific shRNA expression, we crossed shJPH2 mice with αMHC-MerCreMer (MCM) mice, which express a tamoxifen-inducible mutant Cre recombinase under control of the cardiac-specific alpha-myosin heavy chain promoter (αMHC).[15] Tamoxifen administration in double transgenic MCM-shJPH2 mice results in cardiac-specific excision of the *neo* cassette, which activates the U6 promoter and induces expression of JPH2 shRNA (Fig. 1a).

Northern blot analysis confirmed expression of JPH2 shRNA exclusively in the hearts of tamoxifen-injected MCM-shJPH2 mice. Moreover, indicative of the cardiac specificity, there was no JPH2 knockdown in skeletal muscle of tamoxifen-injected MCM-shJPH2 mice (Fig. 1b). Real-time PCR analysis revealed that *JPH2* mRNA levels were significantly lower in hearts of tamoxifen-treated MCM-shJPH2 mice, whereas *JPH1* mRNA levels were unaltered (Fig. 1c). Western blot analysis of cardiac protein lysates demonstrated that knockdown of JPH2 mRNA resulted in a 60% reduction in JPH2 protein (Fig. 1b). Since expression of double stranded RNA might trigger a cellular interferon response with the potential to affect gene expression [16], we measured mRNA levels of oligoadenylate synthase-1 (*OAS1*) and signal transducer and activator of transcription 1 (*STAT1*). Real time PCR analysis demonstrated unaltered levels of *OAS1* and *STAT1* in tamoxifen-treated MCM-shJPH2 mice (Supplemental Fig. 1c). Whereas all provided data were obtained in mice from one transgenic line (line 38), we confirmed similar findings in a second independent shJPH2 transgenic mouse line (line 21) in which JPH2 was reduced by 30% after tamoxifen administration (data not shown). These data show that we successfully created a novel shRNA-mediated approach to selectively reduce JPH2 protein levels in the adult murine heart.

Downregulation of JPH2 Leads to Acute Heart Failure

JPH2 knockdown in MCM-shJPH2 mice caused a significantly reduced survival rate compared to MCM mice (Fig. 1d). Within 1 week after tamoxifen injections, mortality was 40% among MCM-shJPH2 mice compared to 0% among MCM mice ($P=0.004$). Histological analysis of surviving mice revealed cardiac dilatation in MCM-shJPH2 mice (Fig. 1e). Transthoracic echocardiography revealed significantly decreased ejection fractions (EF) in MCM-shJPH2 mice (36.72±4.25%) compared to MCM controls (51.97±2.15%, $P<0.01$) (Fig. 1f; Supplemental Table). Furthermore, end-systolic diameter (ESD) and end-diastolic diameter (EDD) were both significantly larger in MCM-shJPH2 (3.89±0.16 and 4.80±0.07 mm, respectively) compared to MCM control mice (3.19±0.07 and 4.35±0.06, $P<0.001$) (Fig. 1g, h). Similar findings were obtained in MCM-shJPH2 mice from line 21 (Supplemental Table). Left ventricular posterior wall thickness (LVPWd) did not change between MCM-shJPH2 (0.80±0.03 mm) and MCM controls (0.79±0.02 mm; *P*=N.S.;

Supplemental Fig. 1d), suggesting that the observed changes were not due to compensatory cardiac remodeling. Consistently, there was no difference in cardiomyocyte cross sectional areas between MCM-shJPH2 mice and MCM controls (Supplemental Fig. 1e). On the other hand, the lung weight to tibia length ratio was increased in MCM-shJPH2 mice, consistent with pulmonary congestion in MCM-shJPH2 mice (Supplemental Fig. 1f). However, mRNA levels of cardiac stress markers skeletal muscle alpha 1 actin (*Acta1*), atrial natriuretic factor (*ANF*) brain natriuretic peptide (*BNP*), beta myosin heavy chain (*βMHC*) and the exon 4 splice isoform of regulator of calcineurin 1 (*RCAN 1-4*) were not altered after JPH2 knockdown (Supplemental Fig. 1g). Thus, acute loss of JPH2 in the heart results in sudden cardiac death due to acute heart failure in the absence of hypertrophic remodeling.

Loss of Excitation-Contraction Coupling Gain in JPH2 Knockdown Mice

We next determined the effects of JPH2 knockdown on EC coupling by simultaneously measuring VGCC Ca^{2+} influx and RyR2 Ca^{2+} release. Whereas Ca^{2+} influx through VGCC was unaffected by loss of JPH2, Ca^{2+} release from the SR (i.e., Ca^{2+} transients) was significantly smaller in tamoxifen-treated MCM-shJPH2 mice (Fig. 2a). As a result, the gain of EC coupling was reduced by > 50% following JPH2 knockdown (MCM-shJPH2: 0.11±0.02 vs. MCM: 0.29±0.06; $P<0.05$; Fig. 2b). Further analysis revealed that inactivation kinetics (MCM: 35.79 ± 2.53 ms vs. MCM-shJPH2: 31.37 ± 2.18 ms, $P = 0.19$) nor current-voltage relationship of VGCC were affected by loss of JPH2 (Fig. 2c,d). The total amount of Ca^{2+} entering the cell via VGCC was also comparable between MCM-shJPH2 (4.35±0.21 pA/pF) and MCM mice (4.25±0.27 pA/pF; *P*=N.S; Fig. 2e).

In addition to the Ca^{2+} influx trigger, the amount of SR Ca^{2+} release also depends on SR Ca^{2+} load and activity of RyR2 channels. Therefore, we assessed the amount of Ca^{2+} stored in the SR following steady-state pacing at 1 Hz (Fig. 2f). Consistent with EC coupling experiments (Fig. 2a), the amplitude of pacing-evoked Ca^{2+} transients was decreased in MCM-shJPH2 mice (1.91±0.06 F/F0) compared to MCM controls (2.30±0.10, $P<0.01$; Fig. 2g). SR Ca^{2+} content, measured using a caffeine dump protocol, was significantly decreased in MCM-shJPH2 mice (2.92±0.25 F/F0 vs 4.10±0.33, $P<0.01$; Fig. 2h). Surprisingly, however, we observed that the relative amount of SR Ca^{2+} released via RyR2 normalized to SR Ca^{2+} content (i.e., fractional release) was increased when JPH2 was downregulated (Fig. 2i). Since the Ca^{2+} decay curves in the presence of caffeine appeared shallower in MCM-shJPH2 mice compared to MCM controls, we further analyzed NCX activity. Tau values were significantly decreased after JPH2 knockdown ($\tau = 2.70\pm0.23$ for MCM vs. 5.11±0.61 for MCM-shJPH2 mice, respectively ($P<0.01$). Combined, these data suggest that one consequence of JPH2 deficiency is reduced VGCC-RyR2 coupling leading to reduced cardiomyocyte contractility, due to a novel role of JPH2 in directly regulating RyR2 activity.

JPH2 Knockdown Disrupts Junctional Membrane Complex Organization

To ascertain the effects of JPH2 deficiency on the structure of JMCs, we first examined co-localization of VGCC and RyR2 in ventricular myocytes from MCM-shJPH2 mice. Immunofluorescent imaging indicated both types of Ca^{2+} channels were distributed in similar striated patterns (Fig. 3a,d). However, co-localization between the two channels was significantly decreased following JPH2 knockdown, and this was not due to a difference in protein levels (Fig. 3e,f). Thus, loss of JPH2 results in defective co-localization of VGCC and RyR2 Ca^{2+} channels within the JMC.

We therefore examined the structure of transverse (T)-tubules using di-8-ANEPPS staining. A significant disruption of normal T-tubular structure was apparent in cardiomyocytes from tamoxifen-treated MCM-shJPH2 mice (Fig. 4a and Supplemental Fig. 2). These alterations in T-tubular structure did not affect membrane capacitance (average membrane capacitance

= 184.6 ± 22.6 pF for MCM vs. 165.8 ± 22.6 pF for MCM-shJPH2 mice, respectively (P = 0.27)). Transmission electron microscopy was used to investigate ultrastructural changes in the JMCs (Fig. 4b). Cardiomyocytes from MCM-shJPH2 mice had 40% fewer JMCs (0.36 ± 0.04 JMCs/sarcomere) than MCM control mice (0.59 ± 0.01; Fig. 4c). Furthermore, the remaining JMCs were irregular in terms of their structure. Whereas the average distance between the T-tubular membrane and SR membrane was similar (12.45 ± 0.52 nm in MCM-shJPH2 vs. 12.30 ± 0.26 nm in MCM), the gap between the two membranes within a single JMC (intra-dyad width) was more variable in MCM-shJPH2 mice (variance 1.96 nm^2) than in MCM controls (variance 1.21 nm^2, $P<0.01$) (Fig. 4d). In addition, dyad width among different JMCs (inter-dyad width) was significantly more variable in MCM-shJPH2 cardiomyocytes (variance 0.26 nm^2) compared to MCM controls (variance 1.07 nm^2; Fig. 4e). So, acute loss of JPH2 leads to altered morphology and loss of JMCs.

JPH2 Stabilizes the Ryanodine Receptor Ca^{2+} release channel

The reduction in JMC number and disruption of VGCC/RyR2 colocalization could account for the attenuated EC coupling gain (see Fig. 2). However, structural uncoupling of VGCC and RyR2 would theoretically cause reduced RyR2 triggering, leading to increased SR Ca^{2+}. Since we observed the exact opposite, a reduction in SR Ca^{2+} content (Fig. 2f,h), we decided to measure RyR2 channel behavior during cellular diastole in cardiomyocytes from MCM-shJPH2 mice (Fig. 5a,b). Ventricular myocytes of MCM-shJPH2 mice exhibited an increase in cell-wide spontaneous Ca^{2+} release (SCR) events following a 1-Hz pacing train, compared to MCM mice (Fig. 5a,c). Next, we used confocal line scan imaging to visualize Ca^{2+} sparks in isolated cardiomyocytes (Fig. 5b). Knockdown of JPH2 in MCM-shJPH2 mice led to a significantly higher Ca^{2+} spark frequency (Fig. 5b,d). Taken together, our data indicate that loss of JPH2 leads to increased diastolic Ca^{2+} leak via RyR2 channels. Moreover, this suggests that JPH2 is an important RyR2 regulator besides its structural role in the JMC. Immunoprecipitation of RyR2 from mouse heart tissue revealed that JPH2 binds to RyR2, further supporting a novel role of JPH2 in directly regulating RyR2. Thus, our data suggest that JPH2 is required for proper inactivation of RyR2, and that loss of JPH2 can cause diastolic Ca^{2+} leaks.

Effect of JMC Alterations on EC Coupling Gain in a Computational Model

Our experimental data in MCM-shJPH2 mice revealed that acute loss of JPH2 leads to a reduced number of JMCs and an increased variability in the distance between the plasmalemmal and SR membranes. In our *in vivo* model, however, it is not possible to distinguish the individual contributions of these alterations on EC coupling gain, which was severely impaired following JPH2 knockdown. Therefore, we used a mathematical model to quantitatively probe the effects of aforementioned changes in JMC structure within the cardiac myocyte on EC coupling gain (Fig. 6a). The Luo-Rudy (LRd) myocyte simulation model was used, with a modified Ca^{2+} cycling process represented by up to 10,000 discrete Ca^{2+}-release units [17].

Using the exact values for JMC number, inter-dyad, and intra-dyad width variance obtained in the tamoxifen-treated MCM and MCM-shJPH2 mice, the model predicts a 64% drop in EC coupling gain, which is very similar to our *in vivo* measurements (60.0 ± 5.7%; Fig. 6b). First, we simulated the effect of reducing the number of JMCs (or dyads) (Fig. 6c). Our data reveal that a reduction in the number of dyads leads to a reduction in EC coupling gain according to a nearly linear relationship. Subsequently, the effects of changing inter-dyad or intra-dyad width variability were also simulated. In both cases, experimentally observed changes in inter-dyad or intra-dyad width variability (marked in the Figures) were predicted to decrease EC coupling gain (Fig. 6d,e). Finally, we compared the relative contribution of each of these changes in the JMC to the loss of EC coupling gain (Fig. 6f). The reduction in

dyad number was the main contributor, followed by the increase in intra-dyad variability and inter-dyad variability. Combined, these changes account for the severe loss of EC coupling gain, consistent with decreased cardiac contractility observed following JPH2 knockdown.

Rescue of JPH2 Knockdown Phenotype by Overexpression of JPH2

Although shRNA-mediated knockdown of JPH2 expression represents a powerful tool to study the role of JPH2 in the heart, it is theoretically possible that the observed phenotype was due to non-specific side effects of transgene integration or off-target effects of shRNA. Although this seemed less likely without an interferon response and normal mRNA levels of the lesser cardiac JPH isoform (*JPH1*), we performed a series of rescue experiments to further prove the specificity of shRNA-mediated JPH2 knockdown effects. We intercrossed the MCM-shJPH2 mice with transgenic mice overexpressing JPH2 in the heart (OE). Western blot analysis of cardiac lysates revealed supranormal JPH2 levels in tamoxifen-treated MCM-shJPH2-OE triple transgenic mice (Fig. 7a). Echocardiographic analysis revealed that fractional shortening and cardiac dimensions were similar in MCM-shJPH2-OE and MCM mice, suggesting that JPH2 overexpression in hearts of JPH2 knockdown mice rescued cardiac dysfunction (Fig. 7b and Supplemental Table). Furthermore, electron microscopy analysis showed complete rescue of ultrastructural abnormalities, as did confocal imaging of Ca^{2+} transient amplitudes (Fig. 7c,d). Thus, the cardiac phenotype in MCM-shJPH2 mice is specifically caused by shRNA-mediated knockdown of JPH2 in the heart.

DISCUSSION

Proper conversion of plasmalemmal depolarization into release of intracellular Ca^{2+} from the SR is a prerequisite for myocyte contractility [18]. This fundamental process known as Ca^{2+}-induced Ca^{2+} release (CICR) takes place within specialized subcellular domains known as junctional membrane complexes (JMCs). JMCs are found in all excitable cell types, and are believed to be necessary to provide a structural and functional coupling between the plasma membrane and intracellular Ca^{2+} storage organelles such as the SR. In heart failure, the reduced CICR and disorganization of JMC are believed to contribute to contractile dysfunction, although the molecular mechanisms remain poorly understood.

Following the initial discovery of the family of junctophilins (JPH), it was postulated that this class of proteins provides a structural bridge that anchors the SR membrane to the plasmalemma within JMCs. Previous studies in germline JPH2 knockout mice revealed embryonic lethality at E10.5 due to weakened contractility and heart failure.4 Although embryonic JPH2-deficient mice exhibited defective CRUs, it has remained controversial whether this was directly caused by the absence of JPH2, as other knockout mouse models including triadin-deficient mice display similar subcellular defects 19. To overcome these limitations, we developed a novel short hairpin RNA (shRNA)-based interference approach to induce acute knockdown of JPH2 expression levels exclusively in adult mice cardiac myocytes (MCM-shJPH2 mice). Our findings revealed reproducible JPH2 knockdown following tamoxifen administration in two independent transgenic MCM-shJPH2 lines. It is important to highlight that conventional tissue-specific gene knockout only produces heterozygous (50% knockout) and homozygous (100% knockout) genotypes. In contrast, our shRNA-based model allowed us to study a wide range of knockdown percentages in MCM-shHJPH2 mice. Thus, our new approach to inducible and cardiac-specific gene knockdown enabled us to determine the specific role of JPH2 in the maintenance of cardiac structure and function. Specificity of the model was confirmed by demonstrating that transgenic overexpression of JPH2 in MCM-shJPH2 knockdown mice prevented loss of

JPH2 and negated the development of cardiac and cellular phenotypes linked to JPH2 deficiency.

Our findings suggest that loss of JPH2 is directly responsible for impaired cardiac contractility, one of the hallmarks of congestive heart failure. Loss of JPH2 expression in MCM-shJPH2 mice caused development of acute contractile failure in the absence of myocardial remodeling or alterations in expression levels of other Ca^{2+} handling proteins, suggesting that JPH2 deficiency impaired EC coupling within the JMC. Furthermore, our data indicate that loss of cardiac JPH2, as observed in animal models for heart failure [10, 11], is not a compensatory response during heart disease development, but actually plays a causal role in the disease progression. The finding that genetic mutations in *JPH2* cause hypertrophic cardiomyopathy and heart failure also implies a causal link between JPH2 defects and heart disease.[8, 9]

Previous studies in animals with congestive heart failure revealed reduced EC coupling due to an inability of VGCC to trigger sufficient SR Ca^{2+} release [20]. Our findings in cardiomyocytes isolated from MCM-shJPH2 mice suggest that loss of JPH2 expression is directly responsible for defective CICR. Furthermore, JPH2 knockdown in adult cardiomyocytes increased variability in the distance between the SR and PM within a single JMC and among populations of JMCs. These data suggest that the remaining JPH2 proteins are sufficient to keep both membranes together as JMCs, but that the fidelity of JMC morphology is significantly impacted by the loss of JPH2.

The T-tubular system permits the formation of larger numbers of JMCs within cardiomyocytes. T-tubule remodeling has been demonstrated in rats with pressure overload-induced heart failure 21 and patients with congestive heart failure.22 In a recent study, heart failure development was correlated with progressive defects in T-tubule organization and a decline in JPH2 expression levels.[21] Our findings - for the first time - provide a causal link between acute loss of JPH2 in MCM-shJPH2 mice and a reduction in the total number of JMCs and loss of T-tubules in ventricular myocytes. Normalization of the number of JMCs per sarcomere in MCM-shJPH2 mice intercrossed with JPH2 overexpressing (OE) mice further underscores the specific role of JPH2 in maintaining JMC structure. Thus, our data demonstrate that JPH2 is an essential component of the JMC, and that loss of JPH2 leads to disappearance of JMCs within affected cardiomyocytes.

Our studies in cardiomyocytes isolated from JPH2 knockdown mice revealed evidence for spontaneous Ca^{2+} releases from the SR (Fig. 5). Based on findings in embryonic JPH2-deficient mice, it has been previously suggested that impaired coupling between VGCC and RyR2 might lead to impaired emptying of the SR, resulting in overload-induced diastolic SR Ca^{2+} release.[4] However, our findings clearly revealed a reduction in overall SR Ca^{2+} content, which argues against this model (Fig. 2h). Because cardiac RyR2 expression was unaltered following JPH2 knockdown, it is more likely that the loss of JPH2 impairs the ability of RyR2 to remain closed during diastole. The finding that JPH2 can be co-immunoprecipitated using anti-RyR2 antibody is also consistent with direct binding and regulation of RyR2 by JPH2. In fact, defective RyR2 regulation contributes to abnormal Ca^{2+} handling in failing hearts.[23] Thus, our data implicate JPH2 as a new allosteric regulator of RyR2 function, and suggest that JPH2 downregulation can directly impair RyR2 Ca^{2+} release in failing hearts.

Moreover, we found that Ca^{2+}-dependent inactivation (CDI) of VGCC was not altered in MCM-shJPH2 mice, which might be surprising given that the systolic SR Ca^{2+} transient was reduced (Fig. 2). However, it is possible that diastolic SR Ca^{2+} leak due to increased RyR2 leak might elevate diastolic Ca^{2+} levels, thereby normalizing CDI in MCM-shJPH2 mice.

Therefore, it would be interesting to directly measure diastolic Ca^{2+} concentrations in future experiments. Finally, we found that NCX activity was reduced in myocytes from MCM-shJPH2 mice despite unaltered global expression levels. These results suggest that JPH2 might be required for proper subcellular targeting of NCX, but direct evidence for this is currently not available.

we have developed a novel approach to conditionally reduce JPH2 protein levels using RNA interference. Our studies uncovered the physiological roles of JPH2 in cardiac myocytes and implicate JPH2 as an important factor involved in the loss of cardiac contractility in heart failure, a key feature of this prevalent disease. In addition to determining the spacing between the plasmalemma and SR membrane, JPH2 is also required for the structural integrity of JMCs in myocytes. Computational analysis provided further quantitative insights into the relative importance of each of these subcellular defects related to impaired excitation-contraction coupling. Moreover, we found that JPH2 associates with and facilitates RyR2 inactivation, thereby preventing diastolic SR Ca^{2+} leak. This dual functional role for JPH2 in cardiomyocytes may have implications for the development of new therapeutic strategies for heart failure.

Supplementary Material

Refer to Web version on PubMed Central for supplementary material.

Acknowledgments

The authors thank Evelyn Brown and Margaret Gondo for technical assistance with electron microscopy, Dr. Ivone Bruno for assistance with Northern blotting, Dr. Tom Cooper for providing the aMHC plasmid, and Dr. Chu-Xia Deng for providing pBS/U6-LoxP and pBS/U6-ploxPneo plasmids.

FUNDING SOURCES

R.J.v.O. is the recipient of the 2008-2010 American Physiological Society Postdoctoral Fellowship in Physiological Genomics. N.G. is the recipient of a 2010-2012 American Heart Association Predoctoral Fellowship. Y.R. is the Fred Saigh Distinguished Professor at Washington University in St. Louis, and is supported by NIH/NHLBI grants R01-HL033343 and R01-HL049054, and National Science Foundation grant CBET-0929633. A.R.B. is supported by NIH/NEI grants R01-EY017120 and P30=EY007551. M.J.A. is an Established Investigator of the American Heart Association and is supported by NIH grants R01-HD42569 and P01-HL94291, and Mayo Clinic Windland Smith Rice Comprehensive Sudden Cardiac Death Program. X.H.T.W. is a W.M. Keck Foundation Distinguished Young Scholar in Medical Research, and is supported by NIH/NHLBI grants R01-HL089598 and R01-HL091947; Muscular Dystrophy Association grant #69238, and the Fondation Leducq Award to the 'Alliance for Calmodulin Kinase Signaling in Heart Disease'. Y.R., M.J.A., and X.H.T.W. are supported by a Fondation Leducq Award to the 'Alliance for Calmodulin Kinase Signaling in Heart Disease', Any opinions, findings and conclusions or recommendations expressed in this material are those of the authors and do not necessarily reflect the views of the National Science Foundation (NSF).

REFERENCES

1. Bers DM. Cardiac excitation-contraction coupling. Nature 2002;415:198–205. [PubMed: 11805843]
2. Franzini-Armstrong C, Protasi F, Ramesh V. Shape, size, and distribution of Ca^{2+} release units and couplons in skeletal and cardiac muscles. Biophys J 1999;77:1528–1539. [PubMed: 10465763]
3. Song LS, Sobie EA, McCulle S, Lederer WJ, Balke CW, Cheng H. Orphaned ryanodine receptors in the failing heart. Proc Natl Acad Sci U S A 2006;103:4305–4310. [PubMed: 16537526]
4. Takeshima H, Komazaki S, Nishi M, Iino M, Kangawa K. Junctophilins: A novel family of junctional membrane complex proteins. Mol Cell 2000;6:11–22. [PubMed: 10949023]
5. Garbino A, van Oort RJ, Dixit SS, Landstrom AP, Ackerman MJ, Wehrens XH. Molecular evolution of the junctophilin gene family. Physiol Genomics 2009;37:175–186. [PubMed: 19318539]

6. Nishi M, Mizushima A, Nakagawara K, Takeshima H. Characterization of human junctophilin subtype genes. Biochem Biophys Res Commun 2000;273:920–927. [PubMed: 10891348]
7. Ito K, Komazaki S, Sasamoto K, Yoshida M, Nishi M, Kitamura K, Takeshima H. Deficiency of triad junction and contraction in mutant skeletal muscle lacking junctophilin type 1. J Cell Biol 2001;154:1059–1067. [PubMed: 11535622]
8. Landstrom AP, Weisleder N, Batalden KB, Bos JM, Tester DJ, Ommen SR, Wehrens XH, Claycomb WC, Ko JK, Hwang M, Pan Z, Ma J, Ackerman MJ. Mutations in JPH2-encoded junctophilin-2 associated with hypertrophic cardiomyopathy in humans. J Mol Cell Cardiol 2007;42:1026–1035. [PubMed: 17509612]
9. Matsushita Y, Furukawa T, Kasanuki H, Nishibatake M, Kurihara Y, Ikeda A, Kamatani N, Takeshima H, Matsuoka R. Mutation of junctophilin type 2 associated with hypertrophic cardiomyopathy. J Hum Genet 2007;52:543–548. [PubMed: 17476457]
10. Minamisawa S, Oshikawa J, Takeshima H, Hoshijima M, Wang Y, Chien KR, Ishikawa Y, Matsuoka R. Junctophilin type 2 is associated with caveolin-3 and is down-regulated in the hypertrophic and dilated cardiomyopathies. Biochem Biophys Res Commun 2004;325:852–856. [PubMed: 15541368]
11. Xu M, Zhou P, Xu SM, Liu Y, Feng X, Bai SH, Bai Y, Hao XM, Han Q, Zhang Y, Wang SQ. Intermolecular failure of L-type Ca2+ channel and ryanodine receptor signaling in hypertrophy. PLoS Biol 2007;5:e21. [PubMed: 17214508]
12. van Oort RJ, McCauley MD, Dixit SS, Pereira L, Yang Y, Respress JL, Wang Q, De Almeida AC, Skapura DG, Anderson ME, Bers DM, Wehrens XH. Ryanodine receptor phosphorylation by calcium/calmodulin-dependent protein kinase II promotes life-threatening ventricular arrhythmias in mice with heart failure. Circulation 2010;122:2669–2679. [PubMed: 21098440]
13. van Oort RJ, Respress JL, Li N, Reynolds C, De Almeida AC, Skapura DG, De Windt LJ, Wehrens XH. Accelerated development of pressure overload-induced cardiac hypertrophy and dysfunction in an RyR2-R176Q knockin mouse model. Hypertension 2010;55:932–938. [PubMed: 20157052]
14. Coumoul X, Shukla V, Li C, Wang RH, Deng CX. Conditional knockdown of fgfr2 in mice using Cre-Loxp induced RNA interference. Nucleic Acids Res 2005;33:e102. [PubMed: 15987787]
15. Sohal DS, Nghiem M, Crackower MA, Witt SA, Kimball TR, Tymitz KM, Penninger JM, Molkentin JD. Temporally regulated and tissue-specific gene manipulations in the adult and embryonic heart using a tamoxifen-inducible Cre protein. Circ Res 2001;89:20–25. [PubMed: 11440973]
16. Cullen BR. Enhancing and confirming the specificity of rnai experiments. Nat Methods 2006;3:677–681. [PubMed: 16929311]
17. Faber GM, Rudy Y. Action potential and contractility changes in [Na(+)](i) overloaded cardiac myocytes: A simulation study. Biophys J 2000;78:2392–2404. [PubMed: 10777735]
18. Wehrens XH, Lehnart SE, Marks AR. Ryanodine receptor-targeted anti-arrhythmic therapy. Ann N Y Acad Sci 2005;1047:366–375. [PubMed: 16093511]
19. Chopra N, Yang T, Asghari P, Moore ED, Huke S, Akin B, Cattolica RA, Perez CF, Hlaing T, Knollmann-Ritschel BE, Jones LR, Pessah IN, Allen PD, Franzini-Armstrong C, Knollmann BC. Ablation of triadin causes loss of cardiac ca2+ release units, impaired excitation-contraction coupling, and cardiac arrhythmias. Proc Natl Acad Sci U S A 2009;106:7636–7641. [PubMed: 19383796]
20. Gomez AM, Valdivia HH, Cheng H, Lederer MR, Santana LF, Cannell MB, McCune SA, Altschuld RA, Lederer WJ. Defective excitation-contraction coupling in experimental cardiac hypertrophy and heart failure. Science 1997;276:800–806. [PubMed: 9115206]
21. Wei S, Guo A, Chen B, Kutschke W, Xie YP, Zimmerman K, Weiss RM, Anderson ME, Cheng H, Song LS. T-tubule remodeling during transition from hypertrophy to heart failure. Circ Res 2010;107:520–531. [PubMed: 20576937]
22. Ohler A, Weisser-Thomas J, Piacentino V, Houser SR, Tomaselli GF, O'Rourke B. Two-photon laser scanning microscopy of the transverse-axial tubule system in ventricular cardiomyocytes from failing and non-failing human hearts. Cardiol Res Pract 2009;2009:802373. [PubMed: 20224636]

23. Wehrens XH, Lehnart SE, Reiken S, Vest JA, Wronska A, Marks AR. Ryanodine receptor/calcium release channel pka phosphorylation: A critical mediator of heart failure progression. Proc Natl Acad Sci U S A 2006;103:511–518. [PubMed: 16407108]

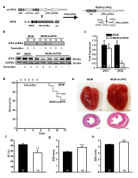

Figure 1. Inducible cardiac-specific JPH2 knockdown causes mortality and acute heart failure

a. Schematic representation of targeting vector to overexpress JPH2-targeting shRNA sequence (shJPH2) downstream of a U6 promoter, inactivated by insertion of a loxP-flanked neomycin (neo) cassette dividing the distal (dU6) and proximal (pU6) parts of the promoter. Tamoxifen administration to double transgenic offspring of αMHC-MerCreMer (MCM) and shJPH2 mice leads to cardiac-specific Cre-mediated excision of the neo cassette, resulting in expression of JPH2 shRNA. **b.** Northern blot analysis (top) of JPH2 shRNA in hearts (H) and skeletal muscle (S) and Western blot analysis (bottom) for JPH2 protein levels in heart lysates from tamoxifen-treated MCM-shJPH2 mice. **c.** Quantitative PCR analysis of JPH1 and JPH2 mRNA levels in cardiac tissue from MCM and MCM-shJPH2 mice. **d.** Kaplan-Meier curve revealing increased mortality in MCM-shJPH2 compared to MCM mice. Arrows indicate single tamoxifen injections at days 1 to 5. **e.** Representative whole mounts (top) and H&E-stained transverse sections (bottom) of MCM and MCM-shJPH2 mouse hearts 1 week after completion of tamoxifen administration. Scale bar = 1 mm. **f, g and h.** Echocardiographic measurement of ejection fraction (EF) (f), end-systolic diameter (ESD) (g), and end-diastolic diameter (EDD) (h) 1 week after tamoxifen. Data are represented as mean ± SEM; * $P<0.05$, ** $P<0.01$, *** $P<0.001$ versus MCM control. Number of mice indicated inside bars.

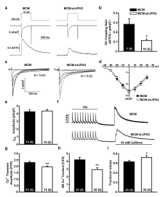

Figure 2. JPH2 knockdown reduces excitation-contraction coupling by suppression of Ca^{2+}-induced Ca^{2+} release

a. Representative simultaneous tracings evoked by a 40 mV depolarization step (upper panel) of Ca^{2+} current through the VGCC (middle panel) and whole cell Ca^{2+} transient (lower panel). **b.** Bar graph of excitation-contraction coupling gain. **c.** Representative whole-cell patch clamp current tracings of amplitude and inactivation kinetics of VGCC. **d.** Current-voltage curves showing activation kinetics of VGCC. **e.** Bar graph showing peak amplitude of Ca^{2+} current through VGCC at 0 mV. **f.** Representative tracings of Ca^{2+} transient amplitudes when paced at 1 Hz and total SR Ca^{2+} content as measured by the amplitude of caffeine-induced Ca^{2+} transient. **g.** Bar graph demonstrating decreased average Ca^{2+} transients in MCM-shJPH2 mice. **h.** Bar graph showing decreased average SR Ca^{2+} load in MCM-shJPH2 mice. **i.** Fractional release (SR Ca^{2+} transient normalized for SR Ca^{2+} load) was increased in MCM-shJPH2 mice. Data are represented as mean ± SEM; numbers indicate total number of cells, with number of mice between brackets; * $P<0.05$, ** $P<0.01$ versus MCM control.

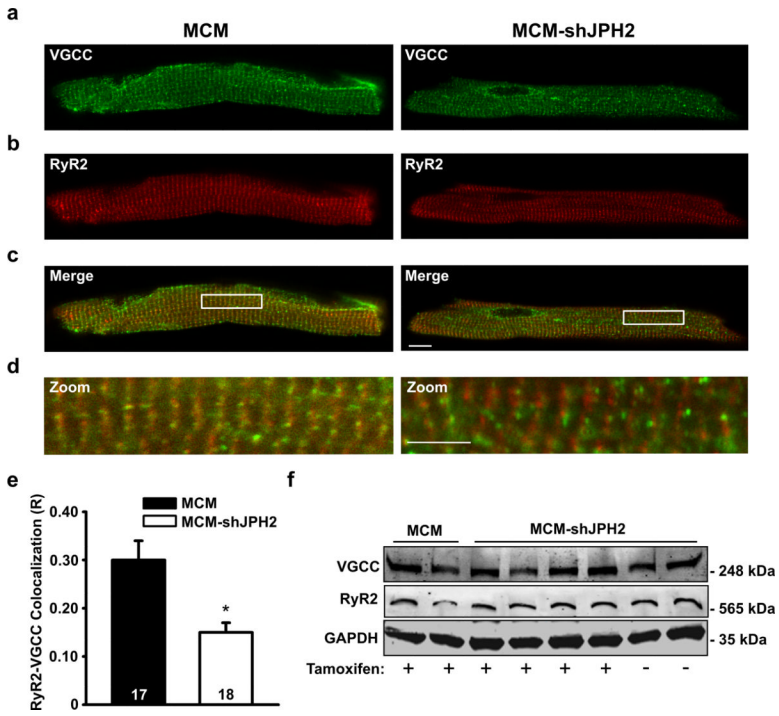

Figure 3. Impaired co-localization of VGCC and RyR2 in cardiomyocytes following JPH2 knockdown

a-c. Representative examples of immunofluorescent labeling of ventricular myocytes isolated from tamoxifen-treated MCM or MCM-shJPH2 mice for VGCC (a), RyR2 (b), and both channels (c). Scale bar = 10 μm. d. Close-ups from images given in panel c demonstrate decreased overlap between VGCC and RyR2 channels in MCM-shJPH2 myocytes. Scale bar = 5 μm. e. Bar graph showing quantification of VGCC-RyR2 co-localization (R), which was significantly reduced following JPH2 knockdown. f. Western blots showing unaltered expression of VGCC and RyR2 following JPH2 knockdown in MCM-shJPH2 mice. Averaged data are represented as mean ± SEM; numbers indicate total number of cells; * $P<0.05$ versus MCM control.

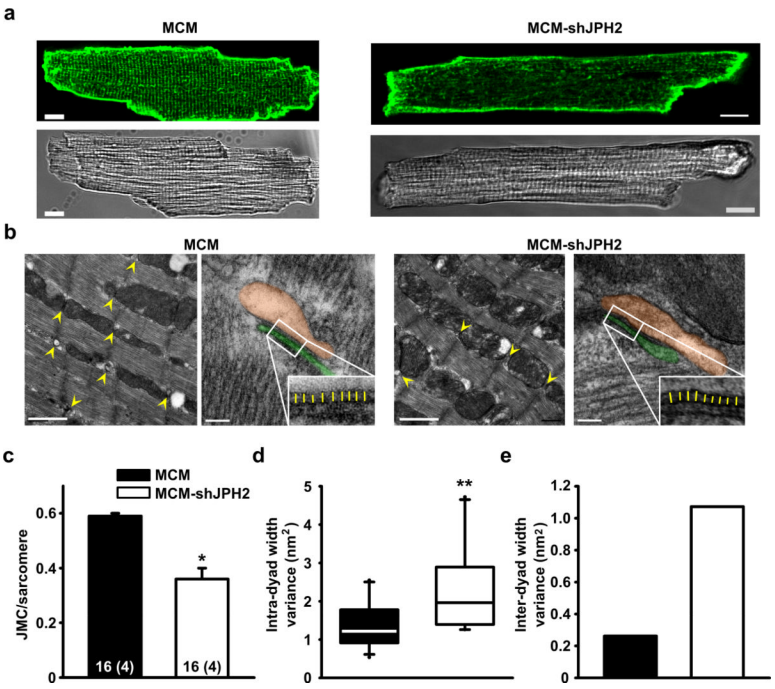

Figure 4. JPH2 knockdown causes fewer but more variable junctional membrane complexes

a. Isolated ventricular myocytes stained with di-8-ANEPPS to visualize T-tubule organization and shown in bright filed. Scale bar = 10 μm **b.** Low magnification electron micrographs of JMCs (yellow arrow heads) in myocytes from MCM-shJPH2 and MCM control mice. Scale bar, 1 μm. High magnification micrographs demonstrate altered morphology of remaining JMCs after JPH2 knockdown (orange pseudocolor indicates SR, and the T-tubule is colored in green). The insets demonstrate more variable distance between SR and T-tubule membranes in MCM-shJPH2 cardiomyocytes (yellow lines). Scale bar, 100 nm. **c.** Quantification of the number of JMCs per sarcomere. **d.** Bar graph showing that the average dyad width variance per JMC was larger in myocytes from MCM-shJPH2 mice. **e**. Bar graph showing overall variance among all measurements of average JMC distance in MCM-shJPH2 versus MCM controls. Averaged data are represented as mean ± SEM; numbers indicate total number of cells, with number of mice between brackets; * $P<0.05$, ** $P<0.01$ versus MCM control.

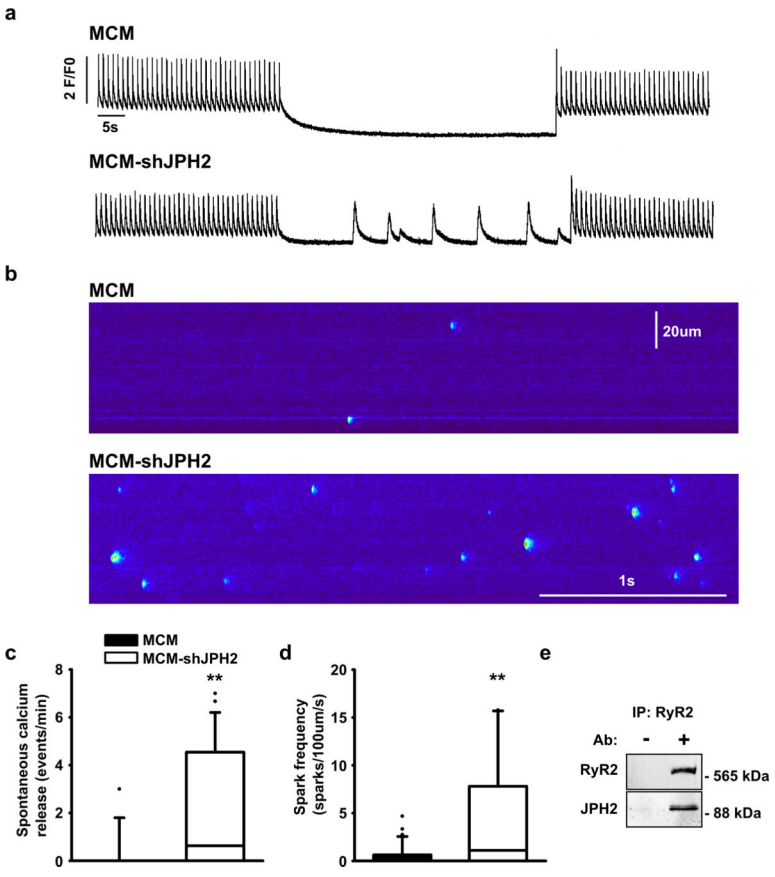

Figure 5. JPH2 knockdown causes defective RyR2 gating resulting in spontaneous SR Ca^{2+} release

a. Representative Ca^{2+} transient recordings demonstrating increased incidence of spontaneous SR Ca^{2+} release events in ventricular myocytes from MCM-shJPH2 mice. **b.** Confocal microscopy line scans revealing increased number of Ca^{2+} sparks in MCM-shJPH2 mice. **c, d**. Box plots showing quantification of the number of spontaneous Ca^{2+} release events (**c**, n=26 cells from 4 mice MCM and 13 cells from 5 mice MCM-shJPH) and Ca^{2+} sparks (**d**, n=37 cells from 4 mice MCM and 28 cells from 5 mice MCM-shJPH). **e**. Co-immunoprecipitation of heart lysates from a wild-type mouse in the presence or absence of anti-RyR2 antibody. Western blots showing that immunoprecitation using anti-RyR2 antibody pulled down JPH2. ** $P<0.01$ versus MCM control.

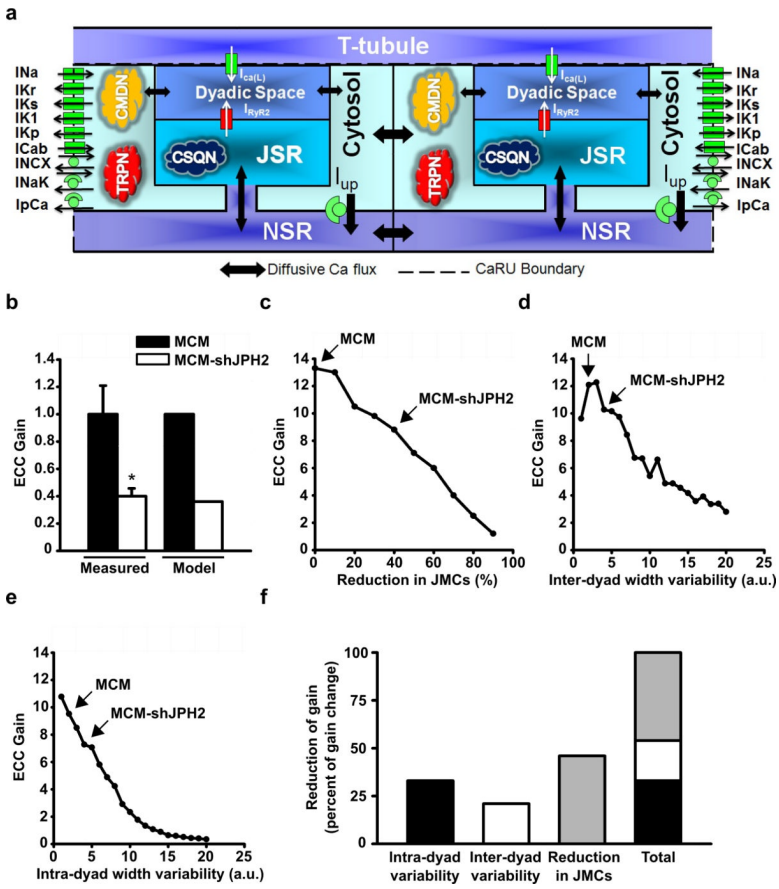

Figure 6. Computational analysis reveals effect of JMC alterations on EC coupling gain

a. Schematic representation of the novel computational model of discrete Ca^{2+} release in a cardiomyocyte. The different Ca^{2+} sources and sinks, as well as the various ion channels and Ca^{2+} binding proteins incorporated in the model are shown. Excitation-contraction (EC) coupling gain is defined as the amount of Ca^{2+} released from the sarcoplasmic reticulum (SR) per unit of Ca^{2+} entering the cell from the extracellular space (T-tubule). **b.** Comparison of EC coupling gain in myocytes from MCM and MCM-shJPH2 mice, as measured using Ca^{2+} imaging (see Figure 2B) and predicted by the computational model. **c-e.** Simulations reveal the effect of a reduced number of junctional membrane complexes (JMCs) (**c**), an increase in inter-dyad width variability (**d**), and an increase in intra-dyad width variability (**e**) on EC coupling gain. Arrows indicate model outcomes for MCM and MCM-shJPH2 mice. **f.** Bar chart showing the individual and cumulative contributions of each parameter on EC coupling gain.

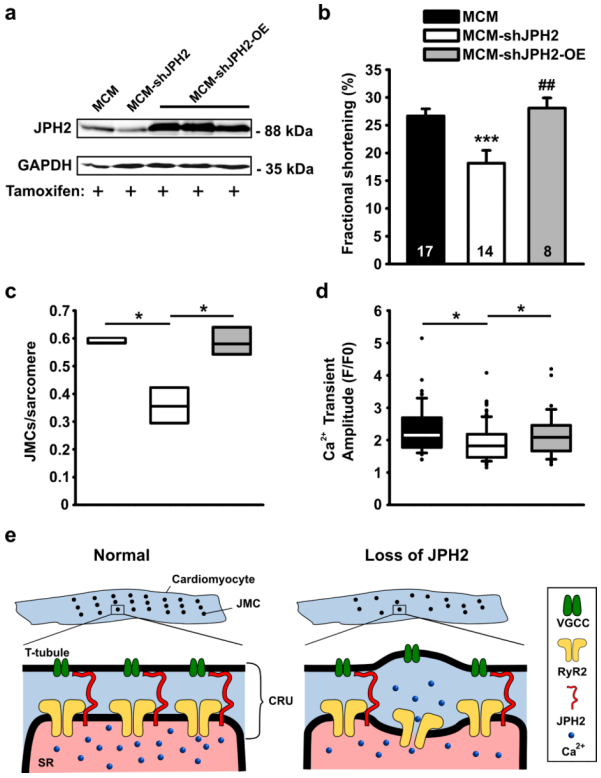

Figure 7. JPH2 knockdown effects can be rescued by transgenic overexpression of JPH2

a. Western blot demonstrating that crossing MCM-shJPH2 mice with transgenic mice overexpressing JPH2 in the heart (OE) restores JPH2 protein to supranormal levels in tamoxifen-treated mice. **b.** Fractional shortening measured using echocardiography. Data are represented as mean ± SEM; number of mice inside bars. **c.** Box plot indicating number of JMCs per sarcomere, as measured by electron microscopy (n=400 sarcomeres per group). **d.** Box plot of Ca^{2+} transient amplitudes measured in isolated cardiomyocytes. **e**. Proposed model of the role of junctophilin-2 (JPH2) in cardiac myocytes. In normal ventricular myocytes (left), junctional membrane complexes (JMCs) are distributed evenly across sarcomeres. Each JMC contains calcium release units (CRU) comprised of voltage-gated Ca^{2+} channels (VCGC) on the sarcolemmal T-tubules, and intracellular Ca^{2+} release channels/ ryanodine receptors (RyR2) on the sarcoplasmic reticulum (SR). Loss of JPH2 expression leads to reduced numbers of functional JMCs per sarcomere, increased variability of the distance between the T-tubule and SR membranes, and defective RyR2 inactivation. * P<0.05, *** P<0.001 versus MCM control, # P<0.05, ## P<0.01 vs MCM-shJPH2.